Arab J Geosci (2014) 7:1993–2005
DOI 10.1007/s12517-013-0924-3

ORIGINAL PAPER

Fission track thermochronology of the Beni Bousera peridotite massif (Internal Rif, Morocco) and the exhumation of ultramafic rocks in the Gibraltar Arc

Ali Azdimousa · Jacques Bourgois · Gérard Poupeau · Mercedes Vázquez · Lahcen Asebriy · Erika Labrin

Received: 21 September 2012 / Accepted: 15 March 2013 / Published online: 12 April 2013

Abstract The Beni Bousera peridotite massif and its metamorphic surrounding rocks have been analyzed by the fission track (FT) method. The aim was to determine the cooling and uplift history of these mantle and associated crustal rocks after the last major metamorphic event that dates back to the Lower Miocene–Upper Oligocene time (~22–24 Ma). The zircon FT analyses give an average cooling—i.e., below 320 °C—age of ~19.5 Ma. In addition, the apatite FT data give an average cooling—i.e., below 110 °C—age of ~15.5 Ma. Taking into account the thermal properties of the different thermochronological systems used in this work, we have estimated a rate of cooling close to 50 °C/Ma. This cooling rate constrains a denudation rate of about ~2 mm year^{-1} from 20 to 15 Ma. These results are similar to those determined in the Ronda peridotite massif of the Betic Cordilleras documenting that some ultrabasic massifs of the internal zones of the two segments of the Gibraltar Arc have a similar evolution. However, Burdigalian sediments occur along the Betic segment (Alozaina area, western Betic segment) unconformably overlying peridotite. At this site, ultramafic rock was exposed to weathering at ages ranging from 20.43 to 15.97 Ma. Since the Beni Bousera peridotite was still at depth until 15.5 Ma, we infer that no simple age projection from massif to massif is possible along the Gibraltar Arc. Moreover, the confined fission track lengths data reveal that a light warming (~100 °C) has reheated the massif during the Late Miocene before the Pliocene–Quaternary tectonic uplift.

Keywords Zircon and apatite fission tracks · Beni Bousera massif · Peridotite exhumation · Miocene · Rif · Betic Cordilleras

A. Azdimousa (✉)
Laboratoire de Géosciences Appliquées, Faculté des Sciences
Université Mohammed 1, Oujda, Morocco
e-mail: azdi61@yahoo.fr

J. Bourgois
Institut des Sciences de la Terre Paris (iSTeP), UMR 7193,
UPMC-CNRS, Université Pierre et Marie Curie, 4 place Jussieu,
75252 Paris Cedex 05, France
e-mail: jacques.bourgois@upmc.fr

G. Poupeau
Centre de Recherche de Physique Appliquée à l'Archéologie et
Institut de Recherche sur les Archéomatériaux, UMR 5060, CNRS
and Université Bordeaux 3, Esplanade des Antilles,
33607 Pessac, France
e-mail: gpoupeau@u-bordeaux3.fr

M. Vázquez
Andean Geothermal Center of Excellence (CEGA),
Universidad de Chile, Santiago, Chile
e-mail: mvazquez@ing.uchile.cl

L. Asebriy
Institut Scientifique, Université Mohammed V,
BP. 704, Rabat-Agdal, Morocco
e-mail: asebriy@israbat.ac.ma

E. Labrin
Laboratoire de Géodynamique des Chaînes Alpines,
UMR 5025, Université Joseph Fourier, Grenoble, France
e-mail: erika.labrin@ujf-grenoble.fr

M. Vázquez
Department of Geology, Universidad de Chile, Santiago, Chile

Introduction

Various segments of the Alpine chains internal zones exhibit major ultramafic bodies such as those extensively described in the French and Italian Alps. Along the Betic–Rif–Tell belts, the Beni Bousera and Ronda massifs border the Alboran coasts of the western Mediterranean Sea (Fig. 1). These peridotite massifs and associated rocks recorded a complex tectonometamorphic history, including high-temperature–(ultra) high-pressure and low-temperature–

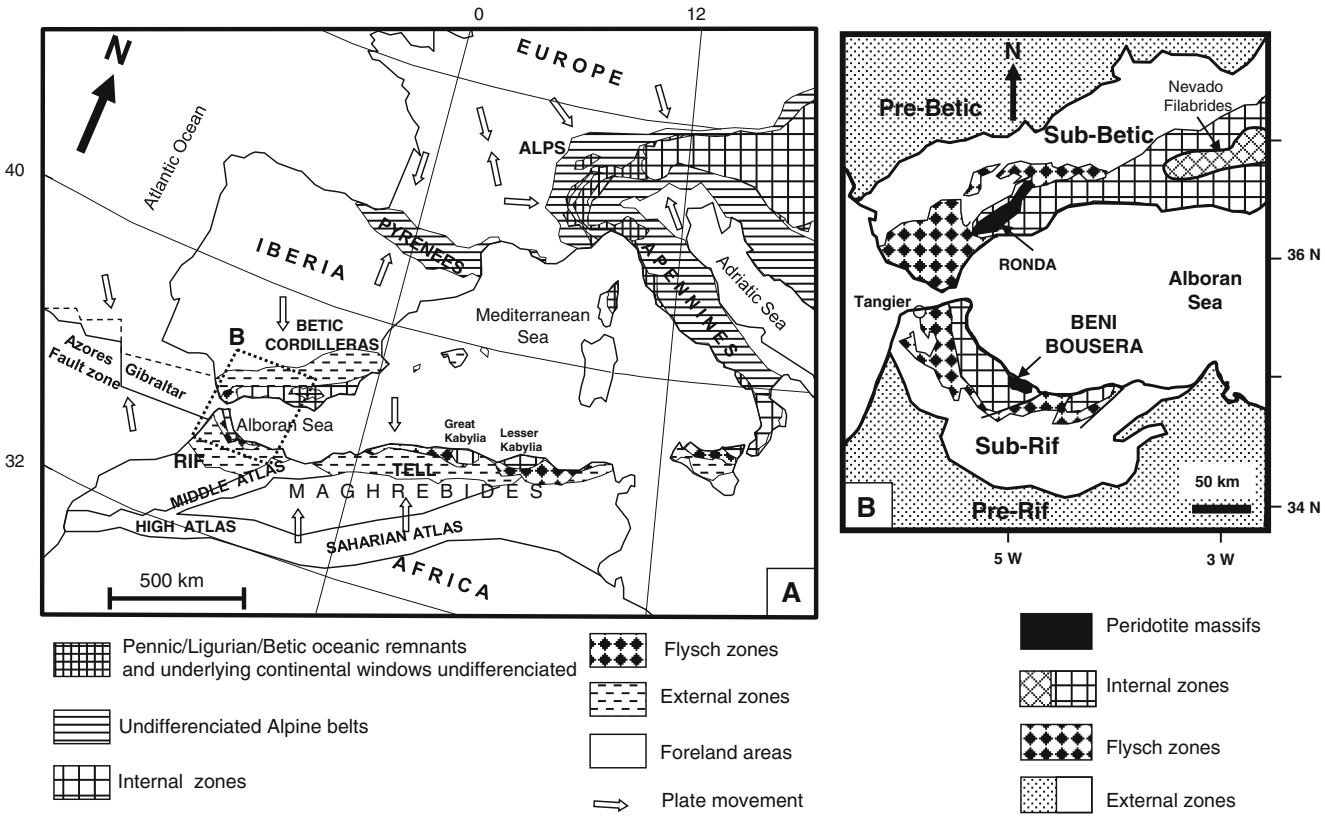

Fig. 1 **a** Regional geological maps of the western Mediterranean area showing the location of the alpine system. **b** Location of the Beni Bousera peridotite massif along the Rif segment bordering the Alboran basin to the south

low-pressure metamorphism. Most often, their exhumation appears to have been related to a major thinning of the crust (Garrido et al. 2011; Beslier et al 1990), or a ductile exhumation associated with the post-orogenic extensional process (Rossetti et al. 2005).

While in the Alps *ss*. and the Betic Cordilleras the latest stages of denudation were investigated by fission track (FT) thermochronology, this was not yet the case for their Maghrebian counterparts. We present here the first FT data obtained for an ultramafic body from the southern branch of the Gibraltar Arc, the Beni Bousera massif. The Arc resulted from the Cenozoic collision between the allochtonous metamorphic terranes of the Alboran Domain and the African and Iberian plates (Andrieux et al. 1971; Balanyá and García-Dueñas 1987; Booth-Rea et al. 2007; Vergés and Fernandez 2012). During the Early and Middle Miocene, the region then underwent a large-scale extensional collapse, accommodated by thin-skinned fold belts at the periphery of the system and by a coeval subsidence along the Alboran Sea basin (Martinez-Garcia et al. 2011 and references therein). The purpose of this work is to contribute to the time/temperature/pressure history of the Beni Bousera massif in the frame of the Gibraltar Arc evolution.

Geological setting

The Rif Chain, which forms the southern branch of the Gibraltar Arc, extends along the North Africa Maghrebian coast. The northern branch of this Arc corresponds to the Betic Cordilleras. Three major zones are usually distinguished within the Rif chain (Bourgois 1978; Chalouan et al. 2008; Vergés and Fernandez 2012), the External Rif, the Flysch units, and the Internal Rif (Fig. 1). The External Rif nappes are mainly composed of sediments deposited along the North African paleomargin during the Mesozoic and the Cenozoic. These rocks exhibit a thin-skinned tectonic style associated locally to a low-grade metamorphism (Andrieux 1971; Frizon de Lamotte 1985; Michard et al. 1992; Asebriy 1994; Asebriy et al. 2003; Azdimousa et al. 1998, 2007; Negro et al. 2006; Booth-Rea et al. 2012).

The Flysch units, also known as Maghrebian Flyschs, originate from the Ligurian–Maghrebian Ocean that connected the Central Atlantic and Alpine Oceans during the Jurassic to the Paleogene times (Durand-Delga and Fontboté 1980; Bouillin 1986; Vergés and Fernandez 2012). These nappes, which mark a suture zone, root beneath the internal zones and overlie the external zones. During the Miocene, part of the Flysch nappes was back-thrusted onto the northern internal zones (Bourgois 1977, 1978; Comas et al 1992; Martinez-Garcia et al. 2013).

The Internal Rif units form part of the Alboran Domain (Andrieux 1971; Balanyá and Garcia-Dueñas 1987). They were interpreted as part of allochthonous terranes thrusting over the Flysch units that, in turn, thrust over the External Rif.

It was proposed that the original paleogeographical location of the internal zones was close to the Kabylian, Peloritanes, and Calabrian internal zones (Wildi 1983; Bouillin 1986; Chalouan 1986). The internal zones of the Betic Cordilleras, as those of Algeria and Italy, were previously proposed as originating from a block detached from northern Africa (Bourgois 1980a, b).

In the studied area (Fig. 2), the Internal Rif exhibits two major tectonic complexes. From base to top, it includes the Sebtide Complex and the Ghomaride nappes. The Ghomaride nappes include Paleozoic sequences structured and metamorphosed during the Variscan orogeny as were the deepest units along the Betic Complex (Gomez-Pugnaire et al. 2012); they are covered by thin remnants of Mesozoic and Cenozoic non-metamorphic rocks (Kornprobst 1969, 1974; Chalouan 1986). Two units were recognized in the Sebtide Complex, the Upper Sebtides, also known as the Federico Units (Milliard 1959), including Carboniferous to Triassic metamorphic rocks (Michard et al. 1983; Bouybaouene 1993) and the Lower Sebtides. The Beni Bousera ultramafic rocks of the Lower Sebtide units exhibit envelopes including, from top to bottom, medium- to high-grade micaschists, gneisses, and kinzigites.

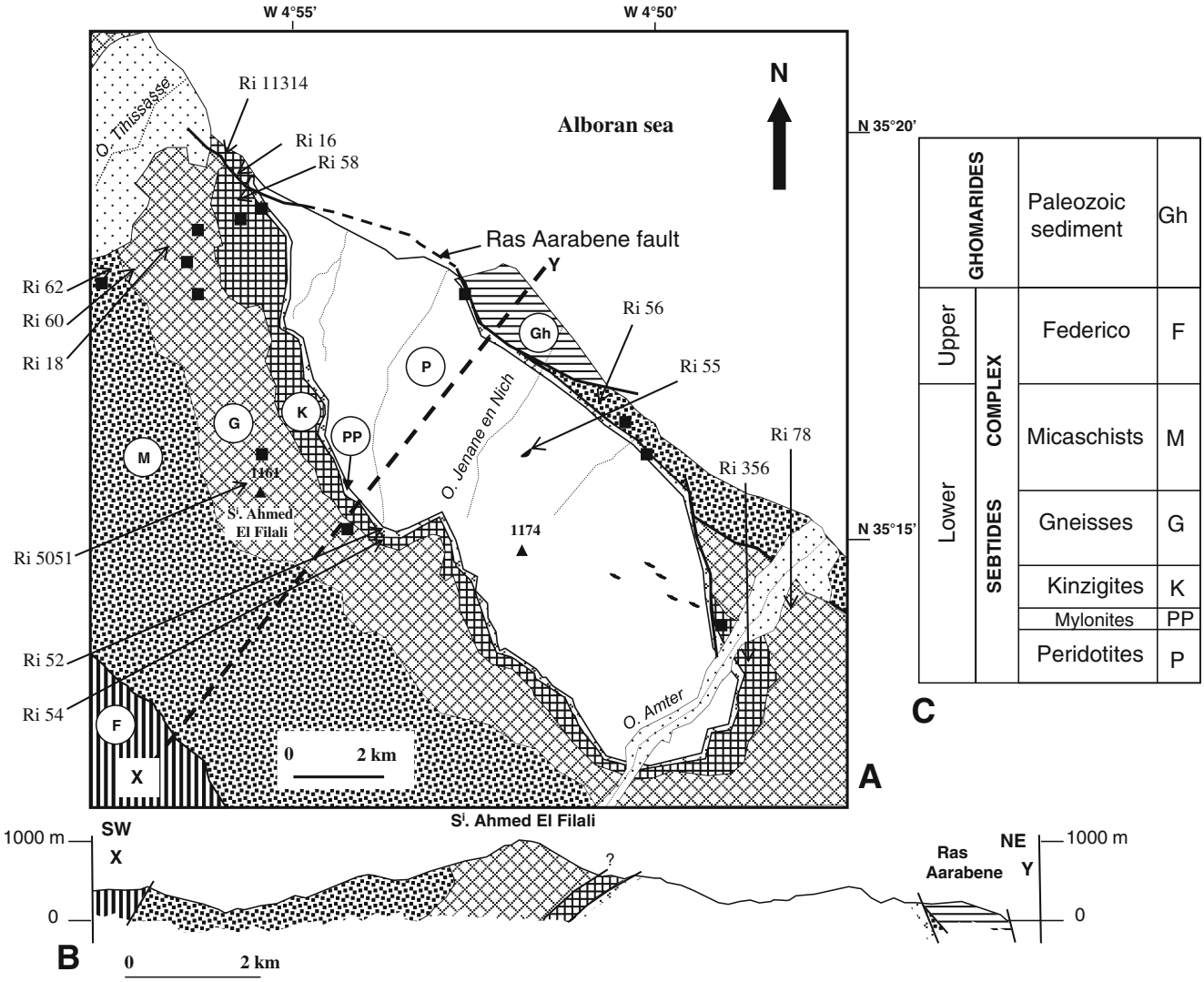

Fig. 2 **a** Simplified geological map of the Beni Bousera massif showing the location of the sampling sites and the location of the cross section of **b**. Note that the Beni Bousera massif exhibits an antiformal structure showing envelopes including kinzigite, gneiss, micaschist, and very low-grade metamorphic rock of the Ghomarides nappes from base to top. **b** General cross section of the Beni Bousera massif, location on **a**. Note the truncation of lower envelopes of the peridotites in relation with the Ras Aarabene normal fault extending along the northern side of the massif. Also note that no significant age variation exists with rock facies, see text for details. *F* Federico unit, *G* gneiss, *Gh* Ghomaride nappes, *K* kinzigite, *M* micaschists, *P* peridotite, *PP* mylonitized zone (pseudoperidotite and serpentinized breaches), *Ri* sample. *Black squares* sterile samples. **c** *Column* showing the succession of major facies exposed in the Beni Bousera area

The age of these rocks emplacement has been strongly discussed. Kornprobst (1974) proposed that it occurred during Hercynian or older times. Subsequently, Loomis (1975), Polvé (1983), Michard et al. (1983), and Garrido et al. (2011) inferred these rocks to be related to the opening of the Alboran Sea during the Oligocene–Lower Miocene times, about 27–21 Ma ago. Using the SHRIMP U-Pb dating technique on zircon, Rossetti et al. (2010) and U–Th–Pb electron microprobe dating on monazite of kinzigites (Montel et al. 2000) documented that the high temperature emplacement of the Beni Bousera peridotite occurred during the Hercynian time. The accordant contact between the peridotite and its kinzigitic envelope, underlined by a mylonite zone and serpentinized breccias, is presumably pre-Alpine in age.

The Beni Bousera massif exhibits lherzolites, harzburgites, dunites, and pyroxenites (Kornprobst 1974; El Maz 1989). Subsequently, leptynite and granite dykes were injected into the peridotites and their surrounding metamorphic cover. Bouybaouene (1993) and Bouybaouene et al. (1995, 1998) describe a HP-LT metamorphism of Alpine age involving the Sebtides rocks similar to the one affecting the Alpujarrides in the Betic chain (Goffé et al. 1989; Tubia and Gil Ibarguchi 1991). This HP-LT metamorphism of rocks covering the peridotites and the associated mineral assemblages were transformed by a subsequent HT metamorphism, which occurred during the Oligocene–Early Miocene times (Michard et al. 1983; Blichert-Toft et al. 1999; Platt et al. 2003a; Garrido et al. 2011). Fluid circulations are associated with these late thermal events that induced a serpentinization and a kelyphytization at the top of the peridotite bodies along the mylonitized zone. This HT metamorphism was related to the Oligo-Miocene extensional phase that produced the Alboran Basin (Platt and Vissers 1989; Platt et al. 2003a; Garrido et al. 2011).

The Beni Bousera ultramafic massif and associated metamorphic envelopes (Fig. 2) exhibit a NW–SE trending dome (Milliard 1959; Kornprobst 1974; Michard et al. 1983). According to Reuber et al. (1982), the intensity of ductile deformation increases toward the peridotites body. Moreover, a stretching lineation is observed in the peridotites with trends ranging from NNW–SSE to NW–SE, although NE–SW trends within the kinzigites or N–S trends in the Federico units were also documented. Isoclinal folds with hinges subparallel to this stretching lineation have been described (Saddiqi 1995; Draoui et al. 1995). The deformation that generated these folds and lineations was associated with simple shear zones exhibiting a top-to-the NNW sense of movement. Brittle deformations are also recognized in the area. On the other side, the main foliation trajectories in peridotites and their overlying crustal units show a systematic rotation toward their mutual contact, indicating a kilometer-scale top to the NW shearing with a dextral component along this crust/mantle contact (Afiri et al. 2011). The low-angle fault bounding the base of the Lower Ghomarides nappe cuts the lower levels of the underlying Sebtides toward the east.

There are two sets of normal faults bounding the peridotite massif. It includes faults parallel to the coastline and a conjugate set of N–S trending faults. The largest of these two faults sets bounds the NE limb of the peridotite dome. It is a high-angle normal fault trending NW–SE that dips seaward toward the northeast. This fault cuts across the internal zone nappe pile including the Sebtides and Ghomarides nappes in the Ras Aarabene area (Fig. 2). Moreover, geophysical models show that the Beni Bousera peridotite branches downward to the mantle (Demnati 1972).

Thermochronometric analysis

Fission track analysis

Twenty-five samples were collected in the Beni Bousera peridotite massif and mainly in its metamorphic envelopes, at elevations ranging from sea level to 1,000 m (Fig. 2). About 3 kg of each rock was crushed. The 80–125-μm-size range was selected for apatite and zircon individual sorting under a stereomicroscope (×20). Thirteen samples have provided enough apatite for dating them. Only four of these 13 samples have provided zircon allowing us to obtain ages. Twelve other samples were found to be sterile (Fig. 2). We assume that the absence of apatite in these samples is related to the extreme abundance of sillimanite. Indeed, the sillimanite has many physical characteristics similar to those of apatite, including the 3.2 density—close to the 3.1 apatite density—the non-fluorescent luminescence, and the transparent to translucent diaphaneity.

The powders Ri11314, Ri5051, Ri356, Ri78, Ri16, Ri18, Ri52, Ri54, Ri55, Ri56, Ri58, Ri60, and Ri62 have provided apatite. Only powders Ri5051, Ri356, Ri78, and Ri18 have also provided zircon. These four samples, which produced both apatite and zircon, include three gneisses (Ri18, Ri78, and Ri5051) and one kinzigite (Ri356). These samples appear to be those where the tracks are discrete indicating an area of total stability—i.e., an area where the tracks acquire their maximum length (15 to 16.3 μm for apatite, 10–13 μm for zircon)—that has suffered an intermediate partial annealing—i.e., a partial annealing zone (PAZ) where the tracks are shorter than in the area of total stability. This PAZ varies between 60 and 120 °C for apatite (Wagner and Van den Haute 1992) and 200 to 320 °C for zircon (Yamada et al. 1995; Tagami et al. 1996; Tagami and Shimada 1996; Tagami 2005; Sueoka et al. 2012). The presence of these two minerals in the same rock is particularly useful for the reconstruction of the thermal history of a massif for temperatures lower than 300 °C.

The fossil tracks were etched in apatites in a solution of HNO3, 1 M volume during 30 to 50 s at room temperature and in zircons using an eutectic melt of NaOH+KOH at 225 °C (Gleadow et al. 1976) during 24–36 h. The dating was performed following the external detector method (Hurford and Green 1983; Hurford and Carter 1991) using the zeta (ζ) technique (Fleischer and Hart 1972; Hurford and Green 1983). According to the conventional analysis of Green (1981), the FT age equation is $t=1/\lambda a\ \ln[1+\lambda a\ \xi\ g\ \rho_m\ (\rho_s/\rho_i)]$; λa is the total (alpha and fission) decay constant for $^{238}U=1.55125\times10^{-10}$ year^{-1} (Jaffey et al. 1971); g is the geometry factor of 0.5 for the external detector method (e.g., Wagner and Van den Haute 1992). ρ_m is the induced fission track density in the standard uranium glass component used as a neutron flux monitor; ρ_s is the spontaneous fission track density of ^{238}U in apatite; ρ_i is the induced fission track density in apatite that is recorded by an external detector.

These densities were obtained after counting N_m, N_s, and N_i tracks counted, respectively, in the monitor, the sample spontaneous fission tracks, and their correlative external detector induced tracks. The standard deviation on the fission track age is calculated taking into account the number of spontaneous fission tracks counted in the sample and the inducted fission tracks counted in the external detector and the monitor glass according to the equation $(\delta t)=t\ [1/N_s+1/N_i+1/N_m+(\delta\xi/\xi)^2]^{1/2}$. In order to objectively test whether there is real variation in single grain ages beyond that expected from track counting alone, Green (1981) and Galbraith (1981) suggested the determination of a chi-squared statistical test (χ^2).

The zeta factor is unique for each observer; its value is specific for a particular standard glass (NIST glass 962, in this work) and is derived empirically from fission track determinations on age standards. For the calibration of these zeta factors, one of us (A. Azdimousa) conducted two irradiations for standard zircon and four for apatite. All irradiations and calibrations were performed in the ORPHÉE nuclear reactor of the *Centre d'Etudes Nucléaires* of Saclay (France). Therefore, the zircon zeta factors are calculated three times for the Buluk Member Tuff (16.2±0.2 Ma; McDougall and Watkins 1985) and seven times for the Fish Canyon Tuff (FCT; 27.8±0.2 Ma; Hurford and Hammerschmidt 1985). These factors are giving us an error weighted mean zeta of ~374±5 (Table 1). Similarly, the calibration of apatite zeta factor gives 317±5 for using three apatite samples of FCT and three others of Durango (31.4±0.3 Ma; Naeser and Fleischer 1975).

Table 1 Determination of the zircon zeta value, using Buluk Member Tuff and Fish Canyon Tuff standards

Sample	ρ_s (N_s)	ρ_i (N_s)	ρ_m (N_m)	Zeta (±1σ)
BMT				
Bul 1	9.76	5.86	0.6011	354±26
	(489)	(320)	(7,155)	
Bul 2	12.69	9.06	0.6313	367±27
	(468)	(334)	(9,351)	
Bul 2	12.69	9.06	0.6313	367±27
	(468)	(334)	(9,351)	
				362±15
FCT				
FCT 1	56.14	23.67	0.6313	370±14
	(2,825)	(1,191)	(9,351)	
FCT 2	61.27	26.83	0.6313	384±13
	(3,214)	(1,407)	(9,351)	
FCT 3	65.18	27.44	0.6313	370±14
	(2,463)	(1,037)	(9,351)	
FCT 4	53.74	22.02	0.6313	360±21
	(1,984)	(690)	(9,351)	
FCT 5	56.39	25.38	0.6313	391±16
	(2,131)	(959)	(9,351)	
FCT 6	64.2	27.68	0.6313	379±15
	(3,432)	(1,480)	(9,351)	
FCT 7	62.6	26.28	0.6313	369±13
	(3,058)	(1,284)	(9,351)	
				376±6
Weighed zeta value				374±5

ρ and N are track densities in 105 tracks/cm^2 and number of tracks counted. The suffix s, i, and d refer to the fossil tracks counted in the crystals and the induced tracks in the external detectors and the NIST glass 962 wafers, respectively

BMT Buluk Member Tuff, *FCT* Fish Canyon Tuff

Results

The results are reported in Table 2. Most of the percent χ^2 values for AFT and ZFT ages pass the 5 % test documenting that most of the obtained individual crystal ages belong to one population in each sample analyzed. So, the apatite fission track ages range from 13.25±1.04 (Ri78) to 17.38±0.63 Ma (Ri16). An average value for apatite ages of ~15.50±1.25 Ma can be considered. For zircons, the ages obtained vary from 18.63±0.65 (Ri18)Ma to 19.34±0.38 Ma (Ri356). The dated zircons allow estimating an average age of ~19.30±1.30 Ma.

In order to determine the final history of cooling, we performed the measurement of confined fission track length (Gleadow et al. 1986) in two apatite samples where the internal track lengths distribution could be determined. The results give 12.78 μm for Ri16 and 13.40 μm for Ri78 (Table 2).

Interpretation

The homogeneous distributions of the zircon individual ages (χ^2 probability test is in general higher than 20 %) suggest that the samples have crossed very fast the retention zone of

Table 2 Fission track data

Sample	Altitude (m)	Mineral	Rock type	Crystals (*n*)	962 NIST ρ_m (N_m)	Spontaneous tracks ρ_s (N_s)	Induced tracks ρ_i (N_i)	Chi-squared probability (%)	FT age ±1σ	Mean track length (μm) (*N*)	SD
Ri 356	35	Z	Kinzigite	31	0.6011 (10,755)	22.25 (6,759)	12.89 (3,915)	36	19.34±0.43		
	35	A	Kinzigite	7	3.532 (13,465)	1.34 (79)	5.37 (318)	56	13.87±1.75		
Ri 52	860	A	Pseudo Peridotite	6	3.776 (9,987)	0.91 (48)	4.37 (177)	95	16.18±2.63		
Ri 55	400	A	Granite	8	3.703 (11,754)	2.604 (192)	9.508 (701)	57	16.02±1.30		
Ri 11314	0	A	Kinzigite	10	3.986 (15,325)	0.67 (764)	2.71 (3,094)	36	15.61±0.63		
Ri 16	150	A	Kinzigite	46	3.592 (9,501)	2.42 (946)	7.95 (3,088)	97	17.38±0.63	12.78 (100)	2.06
Ri 54	800	A	Kinzigite	34	3.776 (9,987)	2.20 (633)	7.62 (2,195)	58	17.20±0.76		
Ri 58	420	A	Kinzigite	32	3.776 (9,987)	1.91 (519)	7.65 (2,073)	36	14.93±0.75		
Ri 78	30	Z	Gneiss	13	0.6011 (10,755)	26.75 (3,407)	15.65 (1,994)	16	19.21±0.57		
	30	A	Gneiss	6	3.986 (15,325)	3.82 (194)	22.03 (1,120)	50	13.25±1.04	13.04 (94)	2.54
Ri 18	200	Z	Gneiss	11	0.6145 (7,314)	19.59 (2,151)	12.03 (1,297)	82	18.63±0.69		
	200	A	Gneiss	54	4.082 (15,325)	1.61 (1,048)	6.55 (4,274)	79	15.82±0.56		
Ri 5051	1,000	Z	Gneiss	14	0.6145 (7,314)	14.61 (2,004)	8.84 (1,213)	28	19.00±0.72		
	1,000	A	Gneiss	9	3.776 (9,987)	1.956 (149)	7.732 (589)	87	15.10±1.38		
Ri 60	100	A	Gneiss	31	3.776 (9,987)	3.14 (826)	10.79 (2,836)	84	17.37±0.69		
Ri 56	260	A	Micaschist	18	3.776 (9,987)	1.96 (299)	7.65 (1,214)	73	14.69±0.97		
Ri 62	40	A	Micaschist	4	3.776 (9,987)	1.12 (38)	4.30 (146)	88	15.52±2.83		

The chi-squared is calculated following Green (1981). The subscripts m refer to the number of induced tracks counted in the 962 NIST monitor, the subscripts s and i to sample spontaneous fission tracks and their correlative external detector induced tracks

A apatite; *Z* zircon; *n* number of crystals; ρ_m, ρ_s, and ρ_i, track densities, in 10^5 t/cm^2 obtained from N_m, N_s, and N_i tracks counted, respectively; *N* the number of confined track lengths measured, *SD* the standard deviation of the confined fission track length

the PAZ between 19 and 20 Ma. These data also document that the Beni Bousera massif was not influenced by a thermal event exceeding 240 °C during the past 19 Ma. In a similar way, apatite FT ages reveal that the PAZ was crossed at 17–14 Ma and that these samples were not re-heated beyond 100 °C since 14 Ma. The zircon and apatite ages support that a very rapid cooling occurred between 19 and 14 Ma. This history and age agree with those proposed for the Alpujarrides in the Betic Cordilleras (Orozco et al. 1998, 2004). Besides, an apatite and zircon FT age-elevation plot shows no clear normal correlation—i.e., between sea level and 1,000 m (Fig. 3). These results evidence that the Beni Bousera dome structure evolved at depth before the final uplift induced by the tensional tectonic phase of the Lower–Middle Miocene. The ductile shearing limiting the kinzigitic gneisses (Kornprobst et al. 1995) must have occurred also at depth, with temperatures higher than 300 °C, which agrees with the deformation temperatures of dry quartz.

The maximum and minimum apatite and zircon FT ages evidence that cooling of the rocks between 300 and 120 °C occurred at rates ranging from 36 to 90 °C/Ma. As these cooling rates took place during the Early Miocene HT extensional event (Platt et al. 2003a), we assume a gradient of 25 to 30 °C/km to calculate the denudation rates. The denudation rates range from 1.4 to1.2 mm/year (minimum) to 3.6 to 3. 0 mm/year (maximum). The maximum values are in good agreement with the 3 km/Ma of exhumation calculated for the Western Betic Cordilleras at 19–20 Ma (Monié et al. 1994). Regarding the Beni Bousera massif, our results indicate that about 6–7 km of the metamorphic rock of the envelope overlying the peridotite has been removed over the past 19–15 Ma. Part of the denudation originated from erosion, providing detrital sediments to the West Alboran Basin (Comas et al. 1992, 1999; Bourgois et al. 1992; Soto et al 1996; Alvarez-Marron 1999; Martinez-Garcia et al. 2013) the deepest depocenter along the Alboran Basin. Indeed, more than 8 km of sediment accumulated in this basin during the Burdigalian to Lower Langhian times. However, part of the denudation originated from a tectonic uplift event related to the Ras Aarabene fault (Fig. 2) that cuts the whole Sebtides Complex. This fault exhibits a 6–8-km minimum extensional displacement that accounts for the main part of the denudation.

Considering that the mean track length is about 13 μm (Table 1), this indicates that they are partially annealed (in our etching condition, the mean track length in Durango apatites is of 14.11±1.26 μm). In Ri16 sample, the percent χ^2 is high enough (97 %) to grant a single age population. An optimization with the Ketcham HeFTy software (2005) was attempted (Fig. 4), keeping in mind that (a) the apatite composition in this sample is unknown and (b) the etching conditions were different. The choice of boxes is changed gradually until the attenuation of conformity between the measured data

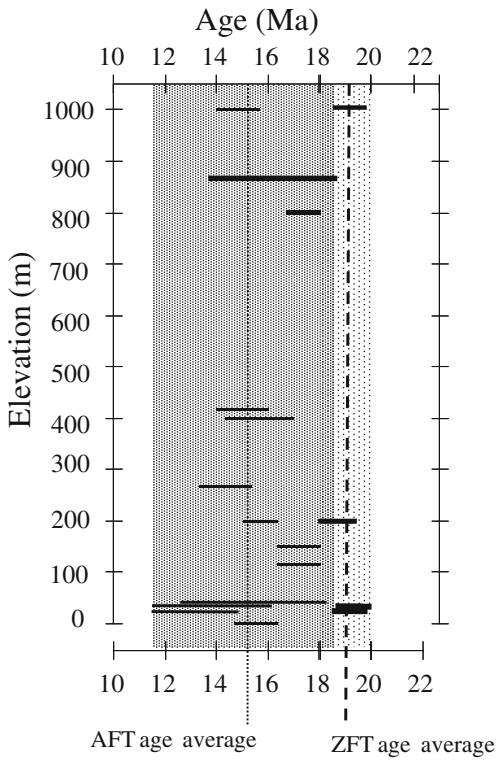

Fig. 3 Comparison between apatite (*AFT*) and zircon (*ZFT*) fission track ages with regard to the elevation of samples. Note that no significant age variation exists in relation with elevation. See text for more detail

(age and length) and the data provided by the model is achieved. The software that provides a best fit of cooling from the GOF parameters calculates the *T–t* pathway. The path is accepted when the GOF is close to 1.

The diagrams of the time–temperature models applied to these samples suggest that after the fast cooling from ~140 to 20 °C, occurring at about 20–17 Ma ago, the massif was progressively reheated to 80 °C between 15 and 5 Ma, before its final cooling and recent denudation. The reheating event was coeval not only with the extensional tectonics that occurred along the Rif Chain at that time but also with the volcanism extending along the Eastern Rif (Hernandez and Bellon 1985). The results of the modeling show also that the final exhumation would be coeval with the Pliocene–Quaternary tectonic uplift that marked the Rif chain. Let us note that similar thermal and exhumation histories have been modeled for the rocks originating from the basement of the Alboran Sea (Hurford et al. 1999).

Thermal and exhumation history

The cooling and uplift history of the Beni Bousera massif presented in this work for temperatures lower than 300 °C

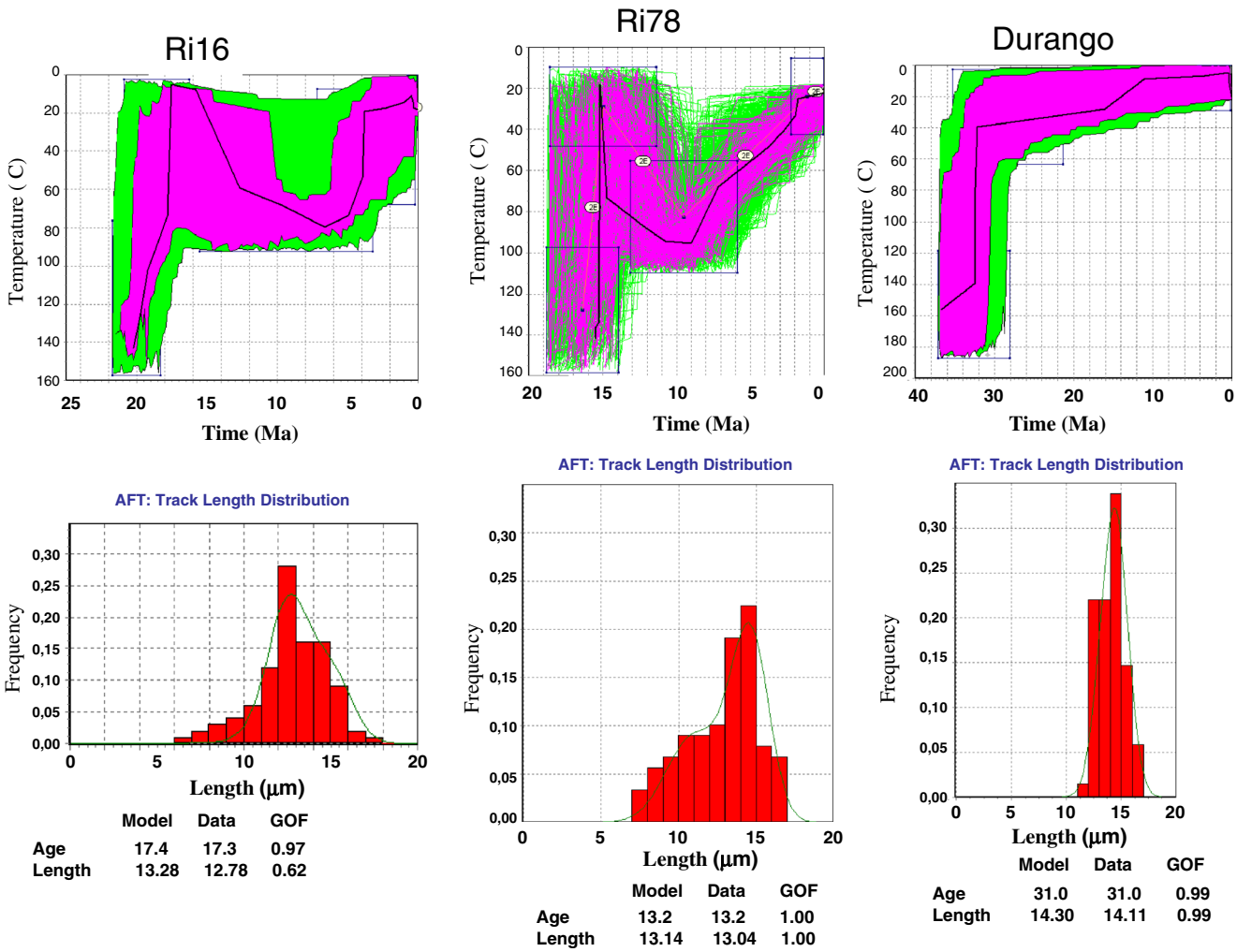

Fig. 4 Diagrams of the time–temperature models performed using HeFTy software (Ketcham 2005) applied to two samples of the Beni Bousera massif (Ri78 and Ri16) in comparison with the mode of cooling of the geological standard of Durango. GOF is the best fit of cooling proposed by the software

can be integrated with the cooling evolution at temperatures higher than 300 °C taking into account the petrological and chronological studies previously published (Fig. 5). According to Davies et al. (1993) and Crespo-Blanc et al. (2006), the peridotites of the Beni Bousera massif originated from the upper mantle (150 km depth, around 1,400 °C and 50 kb). In this sense, the petrologic studies demonstrate that a primary paragenesis had been crystallized at 1,400 °C–25 kb conditions (Kornprobst 1969, 1974). Sanchez-Rodriguez and Gebauer (2000) have proposed that the approximation of the peridotites to the base of the crust would have begun with the Tethys Ocean opening during the Early–Late Jurassic. For the period of convergence between Africa and Europe (Cretaceous to Oligocene), the migration of the Alboran plate toward the west induces a HP metamorphism in the internal units of the Gibraltar arc followed by the subduction of the Tethyan oceanic floor (Van der Wal and Vissers 1993; Azañón et al. 1997; Puga et al. 1995; Davies et al. 1993; Zeck 1996; Chalouan and Michard 2004; Haissen et al. 2004; Michard et al. 2006). The emplacement of the internal zones recorded the Oligocene collision between the various plates. After these compression events, a decompression (Haissen et al. 2004) accompanying the opening of the Alboran basin would have caused again high temperature conditions (~850 °C). The ages obtained by the N_d/S_m method (Polvé 1983), whose closing temperature ranges between 800 and 900 °C as well as the ages obtained by the Lu–Hf (Blichert-Toft et al. 1999) method whose closing temperature exceeds 700 °C (Scherer et al. 2000), allow us to determine that the passage of the isotherms ranging between 900 and 700 °C occurred between 24 and 22 Ma (Figs. 5 and 6).

On the other side, the 22–20-Ma $^{40}Ar/^{39}Ar$ data on biotite (Saddiqi 1995) indicate that the Beni Bousera massif had reached conditions of low pressure and low temperatures (600 to 300 °C) during their uplift toward the surface. Previous data agree with the zircon FT data (20 to 17 Ma) that define a limit age for the last metamorphic event in the

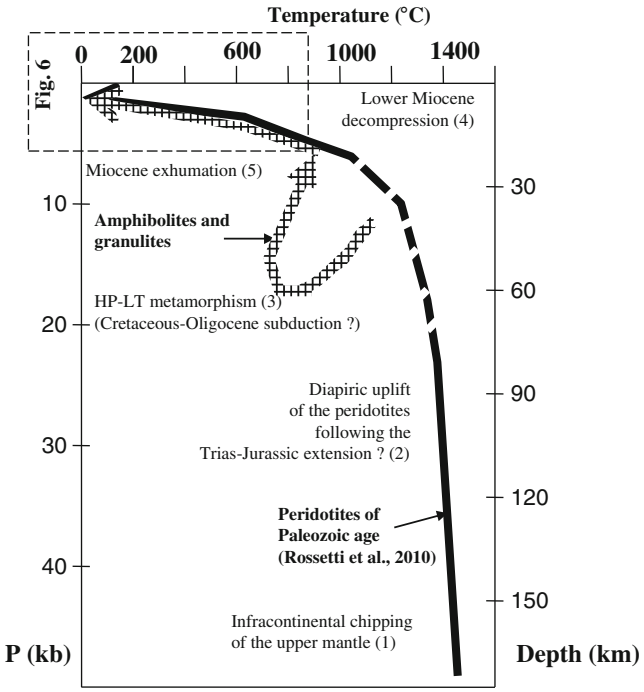

Fig. 5 P–T–t diagram of the Beni Bousera massif, including the available data from published works: (*1*) Davies et al. (1993), Crespo-Blanc et al. (2006); (*2*) Sanchez-Rodriguez and Gebauer (2000); (*3*) Van der Wal and Vissers (1993), Azañón et al. (1997), Puga et al.(1995), Davies et al.(1993), Zeck (1996), Chalouan and Michard (2004), Haissen et al. (2004), Michard et al. 2006); (*4*) Haissen et al. (2004); (*5*) Polvé (1983), Saddiqi (1995), Blichert-Toft et al. (1999), Rossetti et al. (2010), this work

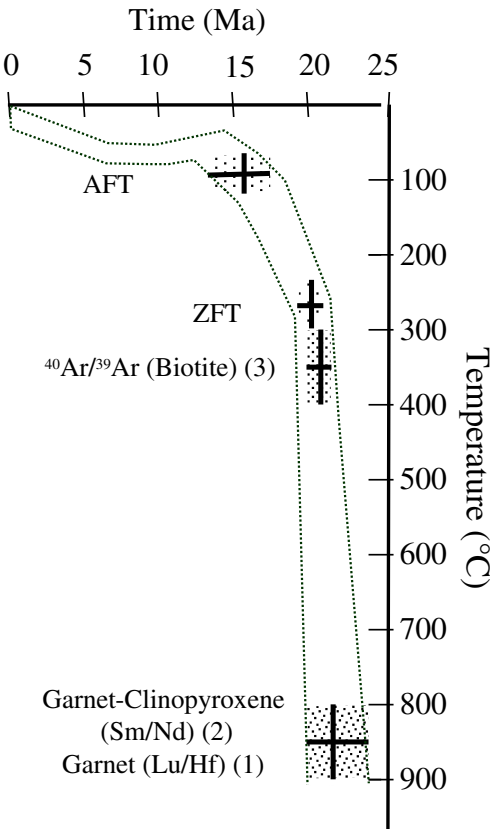

Fig. 6 Temperature versus time diagram of the Beni Bousera massif, including zircon and apatite fission track ages and other thermochronometric data. The cooling diagram shows no main break from 900 to 100 °C that includes the switch from compression- to tensional-related uplift occurring between 25 and 15 Ma. During this time span, the cooling rate is about 80 °C/Ma for the Beni Bousera massif. (*1*) Blichert-Toft et al. (1999); (*2*) Polvé (1983); (*3*) Saddiqi (1995), Rossetti et al. (2010)

internal zones of the Rif that must be older than 20 Ma. In addition, the apatite FT ages (17–14 Ma) mark the cooling stage related to the exhumation of the Beni Bousera sector (Fig. 6).

Consequently, if we combine the apatite and zircon FT ages with the $^{40}Ar/^{39}Ar$ isotopic data of the biotite and take into account also the thermal properties of these thermochronometers, we obtain an average cooling rate of 50 °C/Ma for the period between 20 and 15 Ma. These data document an uplift rate of ~2 mm/year. The comparison of the cooling history of the Beni Bousera massif with the peridotite massifs in the Betic Cordilleras shows that both sectors have undergone a very fast exhumation during the Lower Miocene (Sanchez-Rodriguez and Gebauer 2000; Platt et al. 2003a, 2005; Esteban et al. 2004). The important rates of "tectonic" exhumation in Beni Bousera are close to those observed in the Betic Cordilleras (Priem et al. 1979; De Jong 1991; Zeck et al. 1989, 1992; Monié et al. 1994; Morillon et al. 1996; Sosson et al. 1998; Platt et al. 2003b; Zeck 2004). Finally, the confined length tracks distribution suggests that a light late warming should have occurred in the Beni Bousera massif during the Late Miocene. This warming was probably caused by the crustal thinning at the origin of the volcanism, which occurred in the Western Mediterranean area. These geodynamic events would be synchronous of the African lithosphere delamination during the episode of withdrawal to the west of the oceanic slab of the western Mediterranean (Duggen et al. 2005). In the same way, the modeling of the confined track length distribution shows a fast uplift during the Pliocene and Quaternary times consistent with the regional geology (Fig. 3).

Conclusion and discussion

The zircon FT data obtained in this work document cooling age below 300 °C ranging from 20 to 17 Ma. These ages are slightly younger than the Aquitanian age (Janots et al. 2006; Rossetti et al. 2010) of the last metamorphic event of the Sebtides. Moreover, the apatite FT ages of 17–14 Ma are well correlated with those obtained by FT methods in the Betic Cordilleras (Morillon et al. 1996; Andriessen and Zeck 1996; Platt et al. 2003a, b; Esteban et al. 2003, 2004). Zircon and apatite FT dating associated with other

isotopic dating indicate a rapid cooling associated with a tensional exhumation of the Riffian–Betic internal zones during the Lower–Middle Miocene that post-dated the main metamorphic and tectonic events characterizing the internal zones throughout and the external zones locally (Andrieux 1971; Azdimousa et al. 1998). The tensional-related exhumation phase marked the last tectonic events associated with the individualization of the Gibraltar Arc and the coeval Alboran Sea evolution. The rates of exhumation show that tectonic processes controlled the peridotites denudation during the Lower Miocene. This mode of uplifting was similar to that described in the Betic Cordilleras, suggesting a synchronous and symmetrical tectonic evolution of the two segments of the internal system and coincides reasonably with the model proposed for the Gibraltar arc evolution during the Lower Miocene times (Iribarren et al. 2007).

Several sedimentological and stratigraphic works have documented that the Sebtides/Alpujarrides and Ghomarides/Malaguides nappes were already exposed to weathering by the Early–Middle Burdigalian and Aquitanian ages. It includes (1) the shallow-water Alozaina and Pantano de Andrade Formations of early Burdigalian age, which unconformably overly the Malaguides of Paleozoic age (Bourgois et al. 1971; Bourgois et al. 1972a; Bourgois et al. 1973; Bourgois 1978); (2) the Las Millanas and Viñuela Formations of Burdigalian age, which unconformably overly not only the Malaguides nappes but also the Alpujarrides nappes and associated peridotites (Bourgois et al. 1972b, 1973; Boulin et al. 1973; Bourgois 1978; Serrano et al. 2006). These formations deposited in a shallow to intermediate water depth environment document that all rock facies, including the peridotites, were brought to surficial environment exposed to erosion processes by the Lower Miocene time. Because the Las Millanas Formation unconformably overlies folds involving the Alozaina Formation, Bourgois (1978) assumed that compression shortening stopped by the end of the Aquitanian time as stretching-related tensional tectonics began to control the Alboran basin formation. Following the International Commission on Stratigraphy (Gradstein et al. 2004; Wade et al. 2011), the Las Millanas and Viñuela Formations (Bourgois 1978) extend through the M4 zone, from the lower occurrence of Globoquadrina dehiscens—i.e., astronomical age (Lourens et al. 2004) at 22.44 Ma and geomagnetic polarity time scale at 23.20 Ma (Cande and Kent 1995)—to the highest occurrence of Globigerinita dissimilis—i.e., astronomical age (Lourens et al. 2004) at 17.54 Ma and geomagnetic polarity time scale at 17.62–17.50 Ma (Cande and Kent 1995). In other words, the peridotite massif of the Alozaina area (Betic Cordilleras) was exposed to weathering before 17.62 Ma—i.e., between 23.20 and 17.62 Ma.

Since the Beni Bousera zircon FT ages extend back to 20–18 Ma—i.e., roughly coeval with the age of the unconformity at the base of the Las Millanas and Viñuela Formations—we assume that most of the tectonic uplift recorded by both apatite and zircon cooling ages was tensional-related. The Beni Bousera zircon and apatite FT data document two basic points constraining the evolution of the Beni Bousera antiformal dome: (1) no significant age variation exists in relation with rock facies from the peridotites at the heart of the dome to the micaschist of the most external envelope and (2) no significant age variation exists with elevation between 1,000 m and sea level. We therefore assume that the domal structure formed at depth pre-dating the exhumation through the annealing zircon zone. Accepting a reasonable geothermal gradient ranging from 25 to 30 °C/km, we consider that the Beni Bousera dome structure shaped at depth ranging from 12 to 10 km as a minimum. Whether a cooling rate of 80 °C/Ma (Fig. 6) is accepted, a mean uplift rate of about 2.7 km/Ma acted between 25 and 15 Ma. Since the Beni Bousera peridotite passed through the annealing apatite zone at ~15.5 Ma, an age significantly younger than 17.62 Ma, we assume that ultrabasic rocks were outcropping along the Western Betic Cordilleras (Alozaina area) segment by about 2 Ma earlier. We should consider that the peridotites massifs of the Gibraltar arc evolved through different tectonic history and processes during the time window 20–15 Ma. Because the Beni Bousera peridotites were at ~30 km depth at ~25–22 Ma, we infer that this particular ultramafic body was not the source of detrital material feeding sediment accumulation similar—i.e., the so-called sous-Numidien Formation, NW of the Beni Bousera massif—to that of the Las Millanas-Viñuela Formation.

Acknowledgments We thank the professors A. Jabaloy and G. Booth Rea (Granada University, Spain) for their comments and corrections. We also thank Professor R. A. Ketcham to have placed at our disposal the HeFTy software. The Pierre et Marie Curie University together with the Centre National de la Recherche Scientifique (France) and the Mohammed 1 University of Oujda (Morocco) allowed one of us (J. Bourgois) to be funded for field work.

References

Afiri A, Gueydan F, Pitra P, Essaifi A, Précigout J (2011) Oligo-Miocene exhumation of the Beni-Bousera peridotite through a lithosphere-scale extensional shear zone. Geodin Acta 24:49–60

Alvarez-Marron J (1999) Pliocene to Holocene structure of the eastern Alboran Sea (Western Mediterranean). In: Zahn R, Comas MC, Klaus A (eds) Proceedings of the Ocean Drilling Program, Scientific Results, 161. Ocean Drilling Program, College Station, pp 345–355

Andriessen PAM, Zeck HP (1996) Fission-track constraints on timing of Alpine Nappe emplacement and rates of cooling and exhumation, Torrox area, Betic Cordilleras, S. Spain. Chem Geol 131:199–206

Andrieux J (1971) La structure du Rif central. Notes et Mém Sérv Géol Maroc 235, 155 p

Andrieux J, Fontobé JM, Mattauer M (1971) Sur un modèle explicatif de l'Arc de Gibraltar. Earth Planet Sci Lett 12:191–198

Asebriy L (1994) Evolution tectonique et métamorphique du Rif central (Maroc): définition du domaine Subrifain. Thesis, University of Rabat, Morocco, 284p

Asebriy L, Azdimousa A, Bourgois J (2003) Structure du Rif externe sur la transversale du Massif de Ketama. Trav Inst Sci Rabat Maroc 21:27–46

Azañón JM, Crespo-Blanc A, García-Dueñas V (1997) Continental collision, crustal thinning and nappe forming during the pre-Miocene evolution of the Alpujarride Complex (Alboran Domain, Betics). Struct Geol 19:1055–1071

Azdimousa A, Bourgois J, Poupeau G, Montigny R (1998) Histoire thermique du massif de Kétama (Maroc); sa place en Afrique du Nord et dans les Cordillères Bétiques. CR Acad Sci Paris 326:847–853

Azdimousa A, Jabaloy A, Asebriy L, Booth-Rea G, González-Lodeiro F, Bourgois J (2007) Lithostratigraphy and structure of the Temsamane unit (Eastern external Rif, Morocco). Rev Soc Geol Esp 20(3–4):187–200

Balanyá JC, García-Dueñas V (1987) Les directions structurales dans le Domaine d'Alborán de part et d'autre du Détroit de Gibraltar. CR Acad Sci Paris 304:929–933

Beslier MO, Girardeau J, Boillot G (1990) Kinematics of peridotite emplacement during North Atlantic continental rifting, Galicia, northwest Spain. Tectonophysics 184:321–343

Blichert-Toft J, Albarède F, Kornprobst J (1999) Lu–Hf isotope systematics of garnet pyroxenites from Beni Bousera, Morocco: implications for basalt origin. Science 283:1303–1306

Booth-Rea G, Ranero C, Martínez-Martínez JM, Grevemeyer I (2007) Crustal types and Tertiary tectonic evolution of the Alborán Sea, western Mediterranean. Geochem Geophys Geosyst 8:1–25. doi:10.1029/2007GC001639

Booth-Rea G, Jabaloy-Sánchez A, Azdimousa A, Asebriy L, Vílchez MV, Martínez-Martínez JM (2012) Upper-crustal extension during oblique collision: the Temsamane extensional detachment (eastern Rif, Morocco). Terra Nova. doi:10.1111/j.1365-3121.2012.01089.x

Boulin J, Bourgois J, Chauve P, Durand-Delga M, Magné J, Mathis V, Peyre Y, Rivière M, Antonio Vera J (1973) Age miocène inférieur de la formation de la Vinuela, discordante sur les nappes internes bétiques (Province de Malaga, Espagne). CR Acad Sci Paris 276:1245–1248

Bouillin JP (1986) Le bassin maghrébin: une ancienne limite entre l'Europe et l'Afrique à l'Ouest des Alpes. Bull Soc Geol Fr 8(4):547–558

Bourgois J, Chauve P, Peyre Y (1971) Essai de chronologie des évènements tectono-sédimentaires dans l'Ouest des Cordillères bétiques. CR Somm Soc Géol Fr 8:428–431

Bourgois J, Chauve P, Lorenz C, Monnot J, Peyre Y, Rigo E, Rivière M (1972a) La formation d'Alozaina. Série d'âge oligocène et aquitanien transgressive sur le Bétique de Malaga (région d'Alozaina-Tolox, province de Malaga, Espagne). CR Acad Sci Paris 275:531–534

Bourgois J, Chauve P, Magné J, Monnot J, Peyre Y, Rigo E, Rivière M (1972b) La formation de Las Millanas. Série burdigalienne transgressive, sur les zones internes des Cordillères bétiques occidentales (région d'Alozaina-Tolox, province de Malaga, Espagne). CR Acad Sci Paris 275:169–172

Bourgois J, Chauve P, Peyre Y (1973) Trame de l'histoire post-aquitanienne des Cordillères bétiques occidentales. CR Acad Sci Paris 276:1393–1396

Bourgois J (1977) D'une étape géodynamique majeure dans la Genèse de l'arc de Gibraltar: "l'hispanisation des flyschs rifains au Miocène inférieur". Bull Soc Geol Fr 7:1115–1119

Bourgois J (1978) La transversale de Ronda (Cordillères bétiques, Espagne), Données géologiques pour un modèle d'évolution de l'arc de Gibraltar. Ann Sc Univ Besançon 30, 445 p

Bourgois J (1980a) Pre-Triasic fit and alpine tectonics of continental blocks in the western Mediterranean: discussion and reply. Geol Soc Am Bull 91:632–634

Bourgois J (1980b) De l'origine ultra-bétique des Malaguides (zones internes bétiques, Espagne). Geol Romana 19:151–170

Bourgois J, Mauffret A, Ammar A, Demnati A (1992) Multichannel seismic data imaging of inversion tectonics of the Alboran ridge (western Mediterranean sea). Geo-Mar Lett 12:277–286

Bouybaouene ML (1993) Etude petrologique des metapelites des Sebtides superieures, Rifinteme, Maroc: Une evolution metamorphique de haute pression. Thesis, University of Rabat, Morocco, 150 p

Bouybaouene ML, Goffé B, Michard A (1995) High-pressure, low-temperature metamorphism in the Sebtides nappes, northern Rif, Morocco. Geogaceta 17:117–119

Bouybaouene M, Michard A, Goffé B (1998) High-pressure granulites on top of the Beni Bousera peridotites, Rif belt, Morocco: a record of an ancient thickened crust in the Alboran domain. Bull Soc Géol Fr 169:153–162

Cande S, Kent DV (1995) Rivised calibration of the geomagnetic polarity time scale for the Late Cretaceous and Cenozoic. J Geophys Res 100:6093–6095

Chalouan A (1986) Les nappes ghomarides (Rif septentrional, Maroc). Un terrain varisque dans la chaîne alpine. Thesis, University of Strasbourg, 317p

Chalouan A, Michard A (2004) The Alpine Rif belt (Morocco): a case of mountain building in a subduction–subduction–transform fault triple-junction. Pure Appl Geophys 161:489–519

Chalouan A, Michard A, El Kadiri, Kh, Negro F, Frizon de Lamotte D. Soto J I, Saddiqi O (2008) The Rif Belt. In: Continental evolution: the geology of Morocco; structure, stratigraphy, and tectonics of the Africa–Atlantic–Mediterranean triple junction, vol 116. Springer, Berlin, pp 203–302

Comas MC, Garcia-Dueñas V, Jurado MJ (1992) Neogene tectonic évolution of the Alboran Sea from MCS data. Geo-Mar Lett 12:157–164

Comas MC, Platt JP, Soto JI, Watt SAB (1999) The origin and tectonic history of the Alboran basin: insights from Leg 161 results. In: Zahn R, Comas MC, Klaus A (eds) Proceedings of the Ocean Drilling Program, Scientific Results, vol 161. Ocean Drilling Program, College Station, pp 555–580

Crespo-Blanc A, Luque FJ, Rodas M, Wada H, Gervilla F (2006) Graphite–sulfide deposits in Ronda and Beni Bousera peridotites (Spain and Morocco) and the origin of carbon in mantle-derived rocks. Gondwana Res 9:279–290

Davies GR, Nixon PH, Pearson DG, Obata M (1993) Tectonic implications of graphitized diamonds from the Ronda peridotite massif southern Spain. Geology 21:471–474

De Jong K (1991) Tectono-metamorphic studies and radiometric dating in the Betic Cordilleras (SE Spain): with implications of extension and compression in the western Mediterranean area. Thesis, University of Vrije, Amsterdam

Demnati A (1972) Krustenstruktur im Rif-Bereich von Nord-Marokko aus gravimetrischen und aeromagnetischen Regionalmessungen. Bull Geofis Teor ed Appli 14:203–236

Draoui M, Tabit A, El-Baghdadi M (1995) Mise en évidence d'une structure diapirique déformée au niveau de la partie basale du Massif des Beni-Bousera (Rif interne, Maroc). Geogaceta 17:101–103

Duggen S, Hoernle K, den Bogaard V, Garbe-Schonberg D (2005) Post-collisional transition from subduction- to intraplatetype magmatism in the westernmost Mediterranean: evidence for continental-edge delamination of subcontinental lithosphere. J Petrol 46:1155–1201

Durand-Delga M, Fontboté JM (1980) Le cadre structural de la Méditerranée occidentale. 26th International Geological Congress.

Colloque C5: Géologie des chaînes alpines issues de la Téthys. Mem Bur Rech Geo Min 11:67–85

El Maz A (1989) Le métamorphisme régional méso-catazonal de la série métapelitique de Jbel-Sidi-Mohamed-el Filali, et l'unite granulitique de Beni Bousera (Rif interne), Maroc. Thesis, University of Pierre et Marie Curie, Paris 257 p

Esteban JJ, Cuevas J, Seward D, Tubia JM (2003) Timing of rodingitization at the Ronda peridotites (Betic Cordilleras, Spain). Geogaceta 34:23–26

Esteban JJ, Sánchez-Rodríguez L, Seward D, Cuevas J, Tubía JM (2004) The late thermal history of the Ronda area, southern Spain. Tectonophysics 389:81–92

Fleischer RL, Hart HR (1972) Fission track dating: techniques and problems. In: Bishop W, Miller J, Cole S (eds) Calibration of hominoid evolution. Scottish Academic, Edinburgh, pp 135–170

Frizon de Lamotte D (1985) La structure du Rif oriental (Maroc). Rôle de la tectonique longitudinale et importance des fluides. Mémoires des Sciences de la Terre, University of Paris VI, 436p

Galbraith RF (1981) On statistical models for fission track counts. Math Geol 13:471–488

Garrido CJ, Gueydan F, Booth-Rea G, Precigout J, Hidas K, Padron-Navarta JA, Marchesi C (2011) Garnet lherzolite and garnet-spinel mylonite in the Ronda peridotite: vestiges of Oligocene backarc mantle lithospheric extension in the western Mediterranean. Geology 39:927–930

Gleadow AJW, Hurford AJ, Quaife RD (1976) Fission track dating of zircon: improved etching techniques. Earth Planet Sci Lett 33:273–276

Gleadow AJW, Duddy IR, Green PF, Lovering JF (1986) Confined fission track lengths in apatite—a diagnostic tool for thermal history analysis. Contrib Mineral Petrol 94:405–415

Goffé B, Michard A, Garcıa-Duenas V, Gonzalez-Lodeir F, Monié P, Campos J, Galindo-Zaldivar J, Jabaloy A, Martinez-Martinez JM, Simancas F (1989) First evidence of high pressure, low temperature metamorphism in the Alpujarride nappes, Betic Cordilleras (SE Spain). Eur J Mineral 1:139–142

Gomez-Pugnaire MT, Rubatto D, Fernandez-Soler JM, Jabaloy A, Lopez-Sanchez-Vizcaino V, Gozalez-Lodeiro F, Galindo-Zaldivar J, Padron-Navarta JA (2012) Late Variscan magmatism in the Nevado-Filabride complex: U–Pb geochronologic evidence for the pre-Mesozoic nature of the deepest Betic complex (SE Spain). Lithos 146–147:93–111

Gradstein FM, Ogg JG, Smith AG (eds) (2004) A geologic time scale 2004. Cambridge University Press, Cambridge, 384 p

Green PF (1981) A new look at statistics in fission-track dating. Nucl Tracks 5:77–86

Haissen F, Garcia-Casco A, Torres-Roldan R, Aghzer A (2004) Decompression reactions and P–T conditions in high-pressure granulites from Casares–Los Reales units of the Betic–Rif belt (S Spain and N Morocco). J Afr Earth Sci 39:375–383

Hernandez J, Bellon H (1985) Chronologie K-Ar du volcanisme Miocéne du Rif oriental (Maroc): implications tectoniques et magmatologiques. Rev Géol Dynam Géog Phys 26:85–94

Hurford AJ, Green PF (1983) The zeta age calibration in fission-track dating. Chem Geol Isot Geosci Sect 1:285–317

Hurford AJ, Hammerschmidt K (1985) 40Ar/39Ar dating of the Bischop and Fish Canyon Tufs: calibration ages for fssion-track dating standards. Chem Geol 58:23–32

Hurford AJ, Carter A (1991) The role of fission track dating in discrimination of provenance. In: Morton A, Todd S (eds) Developments in sedimentary provenance studies, vol 57. Geological Society of London, London, pp 67–78

Hurford AJ, Platt JP, Carter A (1999) Fission-track analysis of samples from Alboran Sea basement, ODP Site 976. In: Zahn R, Comas MC, Klaus A (eds) Proceedings Ocean Drilling Program Scientific Results, vol 161. Ocean Drilling Program, College Station, pp 295–300

Iribarren L, Vergés J, Camurri F, Fullea J, Fernàndez M (2007) The structure of the Atlantic–Mediterranean transition zone from the Alboran Sea to the Horseshoe Abyssal Plain (Iberia–Africa plate boundary). Mar Geol 243:97–119

Janots E, Negro F, Brunet F, Goffé B, Engi M, Bouybaouene ML (2006) Evolution of the REE mineralogy in HP–LT metapelites of the Sebtide complex, Rif, Morocco: monazite stability and geochronology. Lithos V 87(3–4):214–234

Jaffey AH, Flynn KF, Glendenin LE, Bentley WC, Essling AM (1971) Precision measurements of the half-lives and specific activities of ^{235}U and ^{238}U. Phys Rev C4:1889–1906

Ketcham RA (2005) Forward and inverse modelling of low-temperature thermochronology data. Rev Mineral Geochem 58:275–314

Kornprobst J (1969) Le massif ultrabasique des Beni Bouchera (Rif interne, Maroc): étude des peridotites de haute température et de haute pression, et des pyroxénites à grnats ou sans grenats, qui leur sont associés. Contrib Mineral Petrol 23:283–322

Kornprobst J (1974) Contribution à l'étude pétrographique et structurale de la zone interne du Rif. Notes Mem Ser Geol Maroc 251, 256p

Kornprobst J, Tabit A, Targuisti K, Draoui M, Woodland AB (1995) A field trip guide for the 2nd International Workshop on Lherzolites and Mantle Processes Granada, Spain, pp 1–50

Loomis TP (1975) Tertiary mantle diapirism, orogeny, and plate tectonics east of the Strait of Gibraltar. Am J Sci 275:1–30

Lourens LJ, Hilgen FJ, Shackleton, NJ, Laskar J, Wilson D (2004) The Neogene Period. In: Gradstein FM, Ogg JG, Smith AG (eds) Geological time scale. Cambridge University Press, Cambridge, pp 409–440

Martinez-Garcia P, Soto JI, Comas M (2011) Recent structures in the Alboran ridge and Yusuf fault zones based on swath bathymetry and sub-bottom profiling: evidence of active tectonics. Geo-Mar Lett 31:19–36

Martinez-Garcia P, Comas M, Soto JI, Lonergan L, Watts AB (2013) Strike-slip tectonics and basin inversion in the Western Mediterranean: the post Messinian evolution of the Alboran Sea. Basin Res. doi:10.1111/bre.12005

McDougall I, Watkins RT (1985) Age of hominoid-bearing sequence at Buluk, northern Kenya. Nature 318:175–178

Michard A, Chlouan A, Montigny R, Ouazzani T (1983) Les nappes cristallophyliennes du Rif (Sebtides, Maroc); témoins d'un édifice alpin de type pennique incluant le manteau supérieur. CR Acad Sci Paris 296:1337–1340

Michard A, Feinberg H, El Azzab D, Bouybaouene M, Sadiqqi O (1992) A serpentinite ridge in a collisional paleomargin setting: the Beni Malek massif, External Rif, Morocco. Earth Planet Sci Lett 113:435–442

Michard A, Negro F, Saddiqi O, Bouybaouene ML, Chalouan A, Montigny R, Goffé B (2006) Pressure–temperature–time constraints on the Maghrebide mountain building: evidence from the Rif–Betic transect (Morocco, Spain), Algerian correlations, and geodynamic implications. C R Geosci 338:92–114

Milliard Y (1959) Les massifs métamorphiques et ultrabasiques de la zone paléozoïque interne du Rif (Maroc). Notes Mém Serv Géol Maroc 147:125–160

Monié P, Torres-Roldán RL, García-Casco A (1994) Cooling and exhumation of the western Betic Cordilleras, $^{40}Ar/^{39}Ar$ thermochronological constraints on a collapsed terrane. Tectonophysics 238:353–379

Montel JM, Kornprobst J, Vielzeuf D (2000) Preservation of old U–Th–Pb ages in shielded monazite; example from the Beni Bousera Hercynian kinzigites (Morocco). J Metamorph Geol 18:335–342

Morillon AC, Bourgois J, Poupeau G, Sosson M (1996) Exhumation au Miocène inférieur des unités Alpujarrides de Los Reales et d'Ojen (Cordillères bétiques, Espagne) à partir de l'étude des traces de fission sur apatites. C Acad Sci Paris 322:885–891

Naeser CW, Fleischer RL (1975) Age of the apatite at Cerro de Mercado, Mexico: A problem for fission track annealing corrections. Geophys Res Lett 2:67–70

Negro F, Beyssac O, Goffé B, Saddiqi O, Bouybaouene ML (2006) Thermal structure of the Alboran Domain in the Rif (northern Morocco) and the Western Betics (southern Spain). Constraints from Raman spectroscopy of carbonaceous material". J Metamorph Geol 24:309–327

Orozco M, Alonso-Chaves FM, Nieto F (1998) Development of large north-facing folds and their relation to crustal extension in the Alboran domain (Alpujarras region, Betic Cordilleras, Spain). Tectonophysics 298:271–295

Orozco M, Alvarez Valero AM, Alonso-Chaves FM, Platt J (2004) Internal structure of a collapsed terrain: the Lujar syncline and its significance for the fold- and sheet-structure of the Alboran Domain (Betic Cordilleras, Spain). Tectonophysics 385:85–104

Platt JP, Vissers RLM (1989) Extensional collapse of thickened continental lithosphere: a working hypothesis for the Alboran Sea and Gibraltar Arc. Geology 17:540–543

Platt JP, Argles TW, Carter A, Kelley SP (2003a) Exhumation of the Ronda peridotite and its crustal envelope: constraints from thermal modelling of a P–T–time array. J Geol Society 160:655–676

Platt JP, Whitehouse MJ, Kelley SP, Carter A, Hollick L (2003b) Simultaneous extensional exhumation across the Alboran basin: implications for the causes of late-orogenic extension. Geology 31:259–262

Platt JP, Kelley SP, Carter A, Orozco M (2005) Timing of tectonic events in the Alpujarride Complex, Betic Cordillera, southern Spain. J Geol Soc London 162: 451–462. doi:10.1144/0016-764903-039

Polvé M (1983) Les isotopes du Nd et du Sr dans les lherzolites orogeniques: contribution à la détermination de la structure et de la dynamique du manteau supérieur. Thesis, University of Paris VII

Priem HNA, Boelrijk NAIM, Hebeda EH, Oen IS, Verdumen EAT, Verschure RH (1979) Isotopic dating of the emplacement of the ultramafic masses in the Serrania de Ronda, southern Spain. Contrib Mineral Petrol 70:103–109

Puga E, Diaz de Federico A, Demant A (1995) The eclogitized pillows of the Betic Ophiolitic Association: relics of the Tethys Ocean floor incorporated in the Alpine chain after subduction. Terra Nova 7(1):31–43

Reuber I, Michard A, Chalcouan A, Juteau T, Jermoumi B (1982) Structure and emplacement of the Alpine type peridotites from Beni Bousera, Rif, Morocco: a polyphase tectonic interpretation. Tectonophysics 82:231–251

Rossetti F, Faccenna C, Crespo-Blanc A (2005) Structural and kinematic constraints to the exhumation of the Alpujarride Complex (Central Betic Cordillera, Spain). J Struct Geol 27:199–216

Rossetti F, Theye T, Lucci F, Bouybaouene ML, Dini A, Gerdes A, Phillips D, Cozzupoli D (2010) Timing and modes of granite magmatism in the core of the Alboran Domain, Rif chain, northern Morocco: implications for the Alpine evolution of the western Mediterranean. Tectonics 29:TC2017. doi:10.1029/2009TC002487

Saddiqi O (1995) Exhumation des roches profondes, péridotites et roches métamorphiques HP-BT, dans deux transects de la chaîne alpine: Arc de Gibraltar et montagnes d'Oman. Thesis, University of Hassan II, Casablaca, Morocco, 245p

Sanchez-Rodriguez L, Gebauer D (2000) Mesozoic formation of pyroxenites and gabbros in the Ronda area (southern Spain), followed by Early Miocene subduction metamorphism and emplacement into the middle crust: U–Pb sensitive high-resolution ion microprobe dating of zircon. Tectonophysics 316:19–44

Scherer EE, Cameron KL, Blichert-Toft J (2000) Lu–Hf garnet geochronology: closure temperature relative to the Sm–Nd system and the effects of trace mineral inclusions. Geochim Cosmochim Acta 64:3413–3432

Serrano F, Sanz de Galdeano C, El Kadiri K, Guerra-Merchan A, Lopez-Garrido AC, Martin-Martin M, Hlila R (2006) Oligocene–Early Miocene cover of the Betic–Rifian Internal Zone. Revision of its geologic significance. Eclogae Geol Helv 99(2):237–253

Sosson M, Morillon AC, Bourgois J, Féraud G, Poupeau G, Saint-Marc P (1998) Late exhumation stages of the Alpujarride Complex (western Betic Cordilleras, Spain): new thermochronological and structural data on Los Reales and Ojén nappes. Tectonophysics 285:253–273

Soto JI, Comas MC, De la Linde J (1996) Espesor de sedimentos en la cuenca de Alborán mediante una conversión sísmica corregida. Geogaceta 20(2):382–385

Sueoka S, Kohn BP, Tagami T, Tsutsumi H, Hasebe N, Tamura A, Arai S (2012) Denudation history of the Kiso Range, central Japan, and its tectonic implications: constraints from low-temperature thermochronology. Island Arc 21:32–52

Tagami T, Shimada C (1996) Natural long-term annealing of the zircon fission-track system around a granitic pluton. J Geophy Res 101:8245–8255

Tagami T, Carter A, Hurford AJ (1996) Natural long-term annealing of the zircon fission-track system in Vienna Basin deep borehole samples: constraints upon the partial annealing zone and closure temperature. Chem Geol 130(1-2):147–157

Tagami T (2005) Zircon fission-track thermochronology and applications to fault studies. Rev Mineral Geoch 58:95–122

Tubía JM, Gil Ibarguchi JI (1991) Eclogites of the Ojen nappe: a record of subduction in the Alpujárride complex (Betic Cordilleras, southern Spain). J Geol Soc London 148:801–804

Van der Wal D, Vissers RLM (1993) Uplift and emplacement of upper mantle rocks in the Western Mediterranean. Geology 21:1119–1122

Vergés J, Fernandez M (2012) Tethys–Atlantic interaction along the Iberia–Africa plate boundary: the Betic–Rif orogenic system. Tectonophysics 579:144–172

Wade BS, Pearson PN, Bergreen WA, Pälike H (2011) Review and revision of Cenozoic tropical planktonic foraminiferal biostratigraphy and calibration to the geomagnetic polarity and asrtronomical time scale. Earth Sci Rev 104:111–142

Wagner GA, Van den Haute P (1992) Fission-track dating. Kluwer Academic, Dordrecht, 285p

Wildi W (1983) La chaîne tello-rifaine (Algérie, Maroc, Tunisie): structure, stratigraphie et évolution du Trias au Miocène. Rev Géol Dynam Géog Phys 24(3):201–297

Yamada R, Tagami T, Nishimura S, Ito H (1995) Annealing kinetics of fission track in zircon: an experimental study. Chem Geol 122:249–258

Zeck HP, Albat F, Hansen BT, Torres-Roldan RL, Garcia Casco A, Martin Algarra A (1989) A 21±2 Ma age for the termination of the ductile Alpine deformation in the internal zone of the Betic Cordilleras, south Spain. Tectonophysics 169:215–220

Zeck HP, Monié P, Villa IM, Hansen BT (1992) Very high rates of cooling and uplift in the Alpine belt of the Betic Cordilleras, southern Spain. Geology 20:79–82

Zeck HP (1996) Betic–Rif orogeny: subduction of Mesozoic Tethys lithosphere under eastward drifting Iberia, slab detachment shortly before 22 Ma, and subsequent uplift and extensional tectonics. Tectonophysics 254:1–16

Zeck HP (2004) Rapid exhumation in the Alpine Belt of the Betic–Rif (W Mediterranean): tectonic extrusion. Pure Appl Geophys 161(3):477–487